TION PAGE

Form Approved
OMB No. 0704-0188

Public reporting burden for this collection of information is estimated to average 1 hour per response, including the time for reviewing instructions, searching existing data sources, gathering and maintaining the data needed, and completing and reviewing the collection of information. Send comments regarding this burden estimate or any other aspect of this collection of information, including suggestions for reducing this burden, to Washington Headquarters Services, Directorate for Information Operations and Reports, 1215 Jefferson Davis Highway, Suite 1204, Arlington, VA 22202-4302, and to the Office of Management and Budget, Paperwork Reduction Project (0704-0188), Washington, DC 20503.

AD-A233 641

1. Agency Use Only (Leave blank).

2. Report Date. 1990

3. Report Type and Dates Covered. Journal Article

4. Title and Subtitle.

Synthetic Temperature Profiles Derived From Geosat Altimetry: Comparison with Air-Dropped Expendable Bathythermograph Profiles

5. Funding Numbers.

Program Element No. 62435N
Project No RM35G84
Task No
Accession No DN256002

6. Author(s).

Michael R. Carnes, Jim L. Mitchell, and P. Webb deWitt

7. Performing Organization Name(s) and Address(es).
Naval Oceanographic and Atmospheric Research Laboratory*
Ocean Science Directorate
Stennis Space Center, MS 39529-5004

8. Performing Organization Report Number.

JA 322:040:89

9. Sponsoring/Monitoring Agency Name(s) and Address(es).

Office of Naval Research
800 North Quincy St., ONR Code 120M
Arlington, VA 22217

10. Sponsoring/Monitoring Agency Report Number.

JA 322:040:89

11. Supplementary Notes.

JGR
*Formerly Naval Ocean Research and Development Activity

12a. Distribution/Availability Statement.

Approved for public release; distribution is unlimitcd.

12b. Distribution Code.

13. Abstract (Maximum 200 words).
Synthetic temperature profiles are computed from altimeter-derived sea surface heights in the Gulf Stream region. The required relationships between surface height (dynamic height at the surface relative to 1000 dbar) and subsurface temperature are provided from regression relationships between dynamic height and amplitudes of empirical orthogonal functions (EOFs) of the vertical structure of temperature derived by deWitt (1987). Relationships were derived for each month of the year from historical temperature and salinity profiles from the region surrounding the Gulf Stream northeast of Cape Hatteras. Sea surface heights are derived using two different geoid estimates, the feature-modeled geoid and the air-dropped expendable bathythermograph (AXBT) geoid, both described by Carnes et al. (1990). The accuracy of the synthetic profiles is assessed by comparison to 21 AXBT profiles sections which were taken during three surveys along 12 Geosat ERM ground tracks nearly contemporaneously with Geosat overflights. The primary error statistic considered is the root-mean-square (rms) difference between AXBT and synthetic isotherm depths. The two sources of error are the EOF relationship and the altimeter-derived surface heights EOF-related and surface height-related errors in synthetic temperature isotherm depth are of comparable magnitude; each translates into about a 60-m rms isotherm depth error, or a combined 80 m to 90 m error for isotherms in the permanent thermocline. EOF-related errors are responsible for the absence of the near-surface warm core of the Gulf Stream and for the reduced volume of Eighteen Degree Water in the upper few hundred meters of (apparently older) cold-core rings in the synthetic profiles.

14. Subject Terms.
(U) Scale Models; (U) Ocean Models

15. Number of Pages. 14

16. Price Code.

17. Security Classification of Report.	18. Security Classification of This Page.	19. Security Classification of Abstract.	20. Limitation of Abstract.
Unclassified	Unclassified	Unclassified	SAR

Synthetic Temperature Profiles Derived From Geosat Altimetry: Comparison With Air-Dropped Expendable Bathythermograph Profiles

MICHAEL R. CARNES, JIM L. MITCHELL AND P. WEBB DEWITT

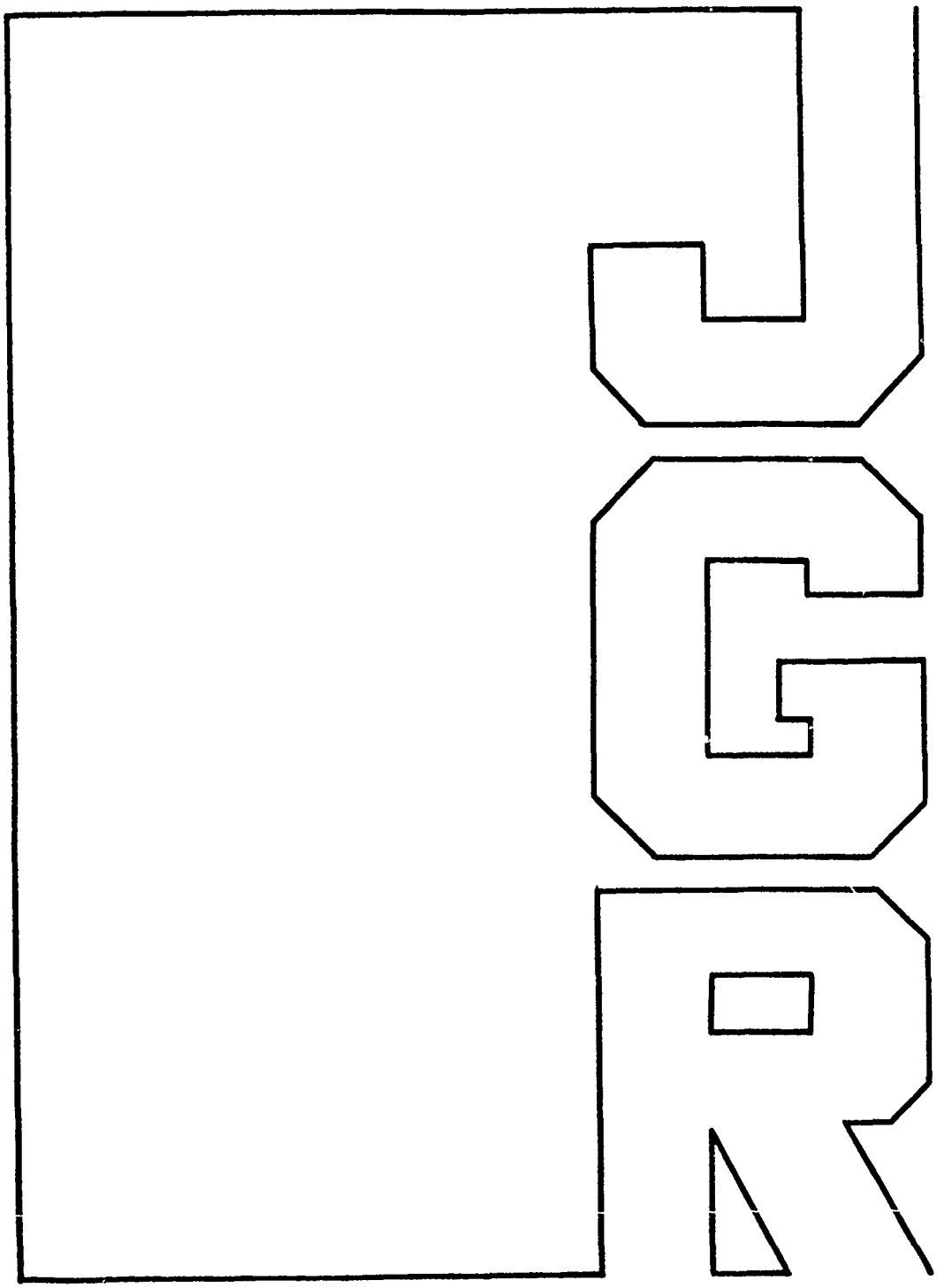

Journal of Geophysical Research, vol. 95, no. C10, Oct. 15, 1990

JOURNAL OF GEOPHYSICAL RESEARCH, VOL. 95, NO. C10, PAGES 17,979–17,992, OCTOBER 15, 1990

Synthetic Temperature Profiles Derived From Geosat Altimetry: Comparison With Air-Dropped Expendable Bathythermograph Profiles

MICHAEL R. CARNES AND JIM L. MITCHELL

Ocean Sensing and Prediction Division, Naval Oceanographic and Atmospheric Research Laboratory, Stennis Space Center, Mississippi

P. WEBB DEWITT

Fleet Numerical Oceanography Center, Monterey, California

Synthetic temperature profiles are computed from altimeter-derived sea surface heights in the Gulf Stream region. The required relationships between surface height (dynamic height at the surface relative to 1000 dbar) and subsurface temperature are provided from regression relationships between dynamic height and amplitudes of empirical orthogonal functions (EOFs) of the vertical structure of temperature derived by deWitt (1987). Relationships were derived for each month of the year from historical temperature and salinity profiles from the region surrounding the Gulf Stream northeast of Cape Hatteras. Sea surface heights are derived using two different geoid estimates, the feature-modeled geoid and the air-dropped expendable bathythermograph (AXBT) geoid, both described by Carnes et al. (1990). The accuracy of the synthetic profiles is assessed by comparison to 21 AXBT profile sections which were taken during three surveys along 12 Geosat ERM ground tracks nearly contemporaneously with Geosat overflights. The primary error statistic considered is the root-mean-square (rms) difference between AXBT and synthetic isotherm depths. The two sources of error are the EOF relationship and the altimeter-derived surface heights. EOF-related and surface height–related errors in synthetic temperature isotherm depth are of comparable magnitude, each translates into about a 60-m rms isotherm depth error, or a combined 80 m to 90 m error for isotherms in the permanent thermocline. EOF-related errors are responsible for the absence of the near-surface warm core of the Gulf Stream and for the reduced volume of Eighteen Degree Water in the upper few hundred meters of (apparently older) cold-core rings in the synthetic profiles. The overall rms difference between surface heights derived from the altimeter and those computed from AXBT profiles is 0.15 dyn m when the feature-modeled geoid is used and 0.19 dyn m when the AXBT geoid is used; the portion attributable to altimeter-derived surface height errors alone is 0.03 dyn m less for each. In most cases, the deeper structure of the Gulf Stream and eddies is reproduced well by vertical sections of synthetic temperature, with largest errors typically in regions of high horizontal gradient such as across rings and the Gulf Stream front.

1. INTRODUCTION

Remote sensing of the ocean surface by satellite-borne sensors now allows rapid worldwide data acquisition. Unfortunately, these measurements provide no direct subsurface information. Strategies for deriving subsurface information from surface measurements are based either on the combination of dynamical models with a moderate amount of historical statistics or are based purely on statistical relationships among historical data. A prime example of the former is the cross-sectional dynamical model of the Gulf Stream with which *Kao* [1987] demonstrated that subsurface density and velocity structure could be accurately computed from satellite altimeter-derived parameters of the sea surface height. *Wunsch and Gaposchkin* [1980] suggest a possible approach to determining the three-dimensional density distribution in the ocean from satellite altimetry based upon a representation of the surface geostrophic pressure field in terms of Rossby wave modes.

Purely statistical relationships between sea surface temperature and subsurface structure [*Khedouri and Szczechowski*, 1983; *Fiedler*, 1988] have shown only marginal success. However, sea surface height has been shown in several statistical studies to be an accurate indicator of subsurface temperature structure. *Cheney* [1982] found that dynamic height anomaly at the sea surface in the northwest Atlantic could be determined within a standard deviation of 9 cm from the depth of either the 15°C or 17°C isotherms. *Khedouri and Szczechowski* [1983] demonstrated the high correlation between the variability of subsurface temperature and dynamic height at the surface.

In an attempt to provide a more complete model of the statistical relationship between surface height and subsurface temperature for the Gulf Stream and Kuroshio regions, *deWitt* [1987] first compiled a data base of all hydrocast (temperature and salinity profiles) in the U.S. Navy's archives. For each monthly data set, he computed the empirical orthogonal functions (EOFs) of the vertical temperature structure and then derived relationships by least squares regression between relative dynamic height and the amplitudes of the first two vertical modes. The first two vertical modes were sufficient to account for more than 95% of the temperature variance in each of the monthly data sets.

This study combines several recent developments to demonstrate and assess the feasibility of generating estimates of temperature profiles (synthetic profiles) in the ocean from measurements made by satellite sensors. The three main components of our approach are the use of processed measurements of the sea surface topography made over

Paper number 90JC00663.

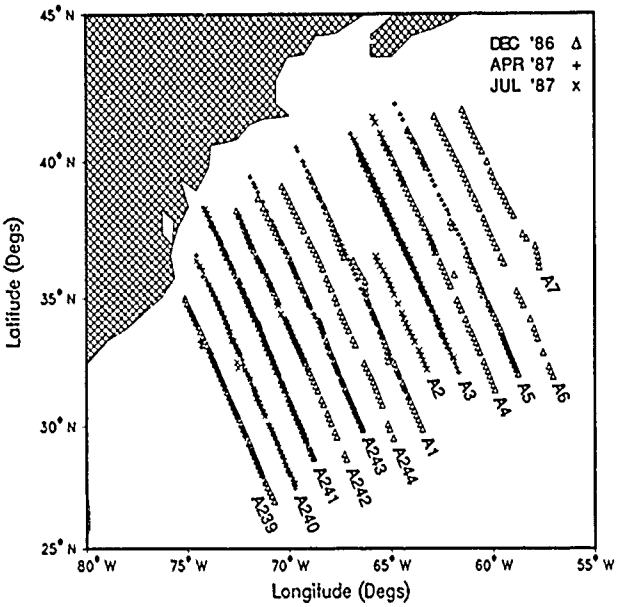

Fig. 1. Chart of the northwest Atlantic showing locations of AXBTs, dropped along Geosat ERM ground tracks, used in this study. Geosat ERM ascending ground tracks are labeled from A1 through A244, beginning with the track over Bermuda and increasing toward the east.

repeated tracks during the Geosat Exact Repeat Mission (ERM) [*Mitchell et al.*, this issue], accurate geoid height profiles along the Geosat ERM ground tracks derived from the combination of altimetry and either air-dropped expendable bathythermograph (AXBT) profiles or feature-modeled fields (M. Carnes et al., unpublished manuscript, 1990 (hereinafter referred to as Carnes et al., 1990)), and an algorithm for constructing temperature profiles from sea surface topography information [deWitt, 1987]. The combination makes possible an assessment of the altimeter in terms of temperature-to-temperature comparisons. Ground truth for sea surface topography derived from altimetry is typically only as accurate as the algorithms for determining absolute dynamic topography from AXBT profiles. An absolute standard does not exist for geoid accuracy determination. However, synthetic temperature profiles can be compared with relatively accurate (the AXBT manfacturer advertises a temperature accuracy of ±0.18°C and depth accuracy of ±2%) AXBT profiles dropped at the time and location of the Geosat altimeter overpass.

2. DATA

AXBTs were dropped along sections through the Gulf Stream and surrounding region during three surveys (December 1986, April 1987, and July 1987) in support of the Naval Ocean Research and Development Activity's (NORDA, now Naval Oceanographic and Atmospheric Research Laboratory, NOARL) Northwest Atlantic Regional Energetics Experiment (REX). AXBTs were dropped at nominal 22-km intervals along Geosat ERM ground tracks within 1 to 2 days of the Geosat overflight. On the April and July surveys, deep (800 m) and shallow (400 m) AXBTs were alternated, but in December only every fourth drop was with a deep probe. Figure 1 is a composite plot for all three surveys showing positions of all AXBTs dropped along Geosat ERM ascending ground tracks. Only ground tracks A241 and A3 have lines of AXBTs from each of the three surveys, and tracks A240, A242, A1, A3, A4, and A5 have two lines each. The remaining five tracks have only one AXBT section (data from track A2 was not used). Ground tracks are numbered consecutively, increasing eastward with track A1 which passes through Bermuda, to a maximum at track A244 just west of A1. Profiles from the April and July surveys are generally of good quality; however, owing to the effects of bad weather, many of the December profiles are excessively noisy at depths greater than 100 m. The noise was reduced by a process of editing and filtering [*Teague*, 1986]. December profiles along ground tracks A1, A241, and A3, are excessively short; for example, the mean depth of profiles along ground track A1 is 256 m with a standard deviation of 92 m.

The three AXBT surveys were conducted during the first year of the Geosat ERM. The time span between the AXBT drops made along a ground track and the Geosat overflight are listed in Table 1 of Carnes et al. (1990). The processing of the raw altimeter sea level (defined as the distance from the sea surface to a reference ellipsoid) data measured along these ground tracks, including editing, smoothing, corrections for ocean tides and EM bias, and long-wavelength radial orbit error correction are presented by *Mitchell et al.* [this issue]. No attempt was made to correct for the oceanic response to atmospheric pressure changes (inverse barometer effect). *Hallock et al.* [1989] determined that the standard deviation of atmospheric pressure at two sites in our study region is about about 7 to 8 mbar. Some studies [e.g., *Byrne and Pullen*, 1983] report using altimeter data corrected for this effect; however, the accepted method [*Tapley et al.*, 1982] is simply to apply a 1-cm correction to sea surface height for each 1 mbar of change in surface atmospheric pressure. The unknown space and time scales of the oceanic response to atmospheric pressure fluctuations make such corrections uncertain at best.

The principal uncorrected source of error is from the integrated water vapor content of the atmosphere. *Hawkins and Smith* [1986] report water vapor–induced altimeter height errors of 10 to 40 cm with space scales of a few hundred kilometers observed in the Gulf Stream region. The short space and time scales and the lack of concurrent measurements by a passive microwave radiometer severly limit capabilities for making water vapor corrections.

3. SYNTHETIC TEMPERATURE PROFILES

The statistical relationship between dynamic height at the surface and temperature at standard depths were constructed by *deWitt* [1987] from an edited data set consisting of all available temperature and salinity hydrocasts from the Master Oceanographic Observation Data Set maintained by the Naval Oceanographic Office for the area bounded by 35°N to 40°N and by 60°W to 75°W. Profiles were assembled into monthly subsets and interpolated to 17 standard depths from the surface to 1000 m. Too few profiles extended past 1000 m to allow use of deeper standard depths. The first two empirical orthogonal functions ϕ_n of the vertical structure of temperature were computed, and the corresponding amplitudes A_n for each mode were determined for each cast. The mean temperature profile and the first two EOFs for July are shown in Figure 2. Profiles in other months are similar

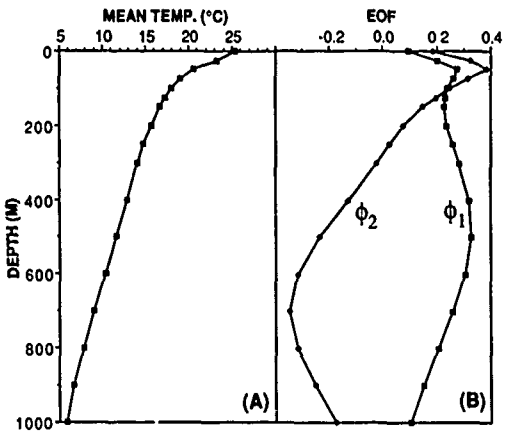

Fig. 2. Profiles versus depth for July of (*a*) the mean temperature and (*b*) the first two EOFs computed from the Gulf Stream region data set by *deWitt* [1987].

TABLE 1. Number of Profiles in Each Monthly Data Set Used in the Calculation of EOFs and Amplitudes, and the Coefficient of Determination (r^2) for the Third-Order Least Squares Fits of EOF Amplitudes A_1 and A_2 [from *deWitt*, 1987]

Month	Number of Profiles	r^2	
		A_1	A_2
Jan.	114	0.97	0.05
Feb.	72	0.97	0.14
March	68	0.80	0.02
April	137	0.97	0.03
May	193	0.97	0.14
June	187	0.98	0.07
July	253	0.98	0.14
Aug.	297	0.96	0.13
Sept.	206	0.97	0.17
Oct.	236	0.97	0.20
Nov.	172	0.98	0.22
Dec.	98	0.97	0.12

except in the upper 100 m. The amplitudes of the first and second EOFs are plotted versus dynamic height (0/1000 dbar) in Figures 3*a* and 3*b*. The first EOF provides the primary temperature change across the Gulf Stream; its amplitude is a nearly a linear function of dynamic height and is zero near the center of the stream, producing colder water throughout the water column at lower heights and warmer water at greater heights. The second EOF provides the warmer near-surface water of the Gulf Stream; its amplitude reaches a maximum near the center of the Gulf Stream, increasing temperatures by 2°C to 4°C in the upper 100 m and lowering temperatures below about 250 m. The increased lateral uniformity of near-surface temperatures during summer is reflected by the decreased values of both EOF profiles in the upper 50 m. The EOF amplitudes were fitted [*deWitt*, 1987] by least squares regression with third-order polynomials. The resulting relationships allow calculation of the temperature estimate $\theta(z_k)$, referred to as synthetic temperature, at any standard depth z_k to be computed from the given surface topography d according to

$$\theta(z_k) = \bar{\theta}(z_k) + \sum_{n=1}^{2} A_n(d)\phi_n(z_k) \quad (1)$$

$$A_n(d) = b_{0n} + b_{1n}d + b_{2n}d^2 + b_{3n}d^3 \quad (2)$$

where ϕ_n are the eigenfunctions, b_0, b_1, b_2, and b_3 are regression coefficients, $\bar{\theta}(z_k)$ is the monthly mean temperature profile, and the subscript k is the depth index. The regression model amplitudes curves are plotted over the data in Figure 3. The coefficient of determination (r^2), a measure of the proportional reduction in variability of the dependent variable (A_n) by the regression model, is listed for each month for both the A_1 and A_2 models in Table 1. As is demonstrated in Figure 3*a*, the first-mode regression fits are excellent, accounting for at least 96% of the amplitude variance in all months except March. The regression model is a much poorer fit (r^2 from 0.05 to 0.22) for the second EOF amplitudes. The use of third-order polynomials by *deWitt* [1987] is justified by tests of significance in most cases for A_2, but only second-order polynomials are justified for A_1.

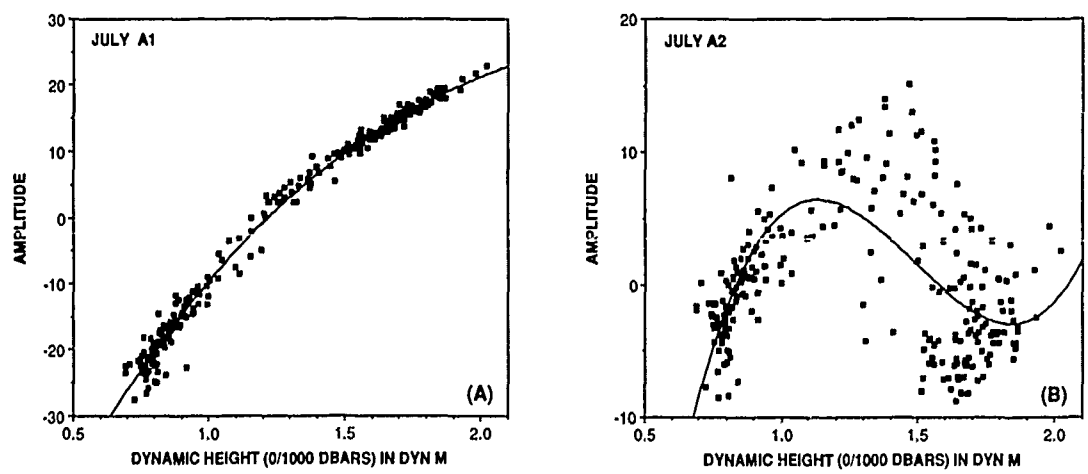

Fig. 3. Amplitudes versus dynamic height of (*a*) the first and (*b*) the second EOFs computed for each temperature profile from the July historical data set used by *deWitt* [1987], and curves of the third-order polynomial least squares fits.

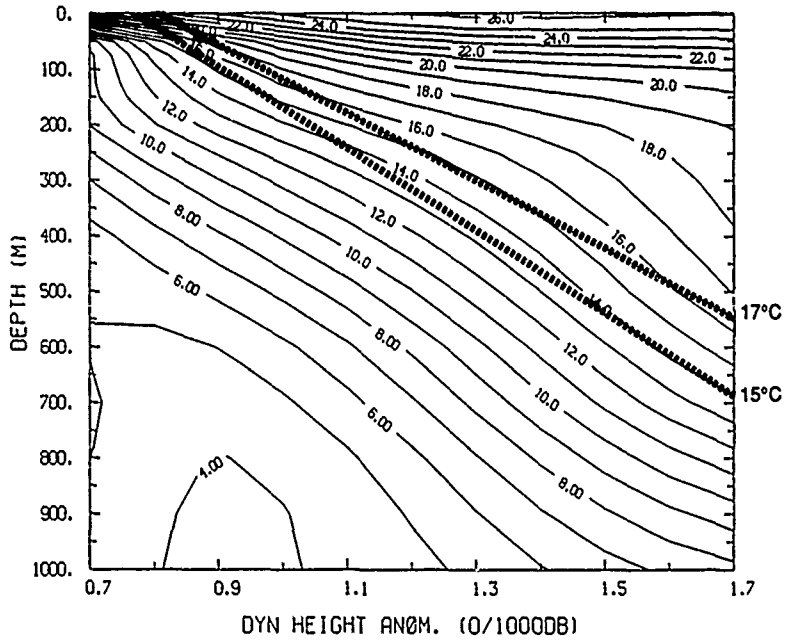

Fig. 4. Synthetic temperature (in degrees Celsius) versus depth and dynamic height (0/1000 dbar) computed from the EOF relationships for July.

However, he retains the third-order equations for all models because they produce more reasonable reconstructed temperature profiles, when compared to the true profiles, than do quadratic models. Clearly, however, there is danger of overfitting the data, as is demonstrated in Figure 3*b*.

Some of the characteristics of synthetic temperature profiles computed from the EOFs and regression relationships derived by *deWitt* [1987] will be examined next. A contour plot of synthetic temperature versus depth and surface dynamic height (0/1000 dbar) is shown in Figure 4 for the month of July. Similar plots for other months differ, primarily, only in the upper 200 m. The north wall of the Gulf Stream is near the 1.1 dyn m level according to the widely used definition of the point where the 15°C isotherm passes the 200-m depth level [*Leitao et al.*, 1979]. The nearly linear relationship between isotherm depth and dynamic height over portions of the field has been recognized in several previous studies [*Khedouri and Szczechowski*, 1983; *Bernstein et al.*, 1982; *Cheney*, 1982] and used to determine dynamic height from temperature profiles. The linear relationship between dynamic height and the depths of the 15°C and 17°C isotherms used by *Mitchell et al.* [this issue] is

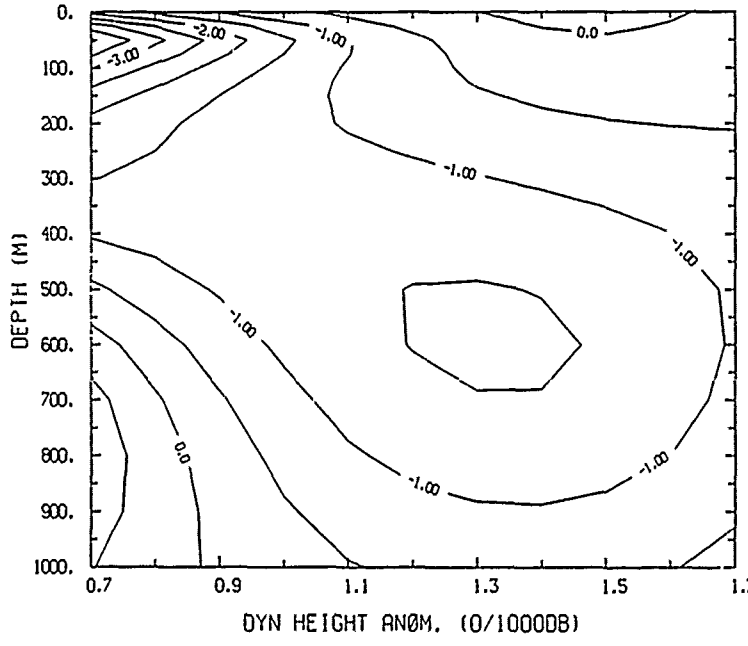

Fig. 5. Synthetic temperature offset produced by the EOF relationships for July resulting from a 0.10 dyn m offset in relative dynamic height, plotted versus depth and dynamic height.

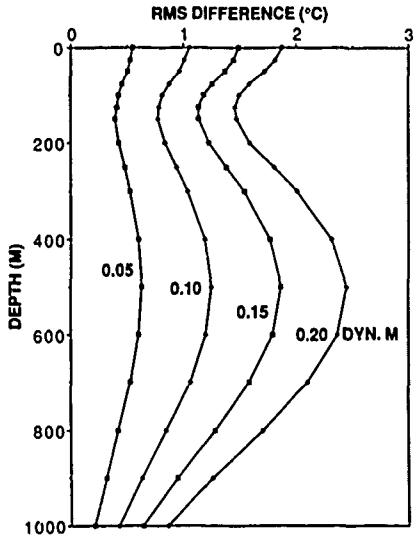

Fig. 6. Profiles of the rms synthetic temperature offset versus depth produced by relative dynamic height offsets of 0.05, 0.10, 0.15, and 0.20 dyn m.

shown in Figure 4. The synthetic isotherm depths are generally shallower than regression isotherm depths by as much as 100 m for the 15°C isotherm and 140 m for the 17°C isotherm, with greatest differences across the Gulf Stream.

An example of the sensitivity of the synthetic temperature algorithm to errors in dynamic height has been prepared in Figure 5, again for July, by computing the temperature difference caused by a 0.10 dyn m offset in dynamic height. The largest differences are near the surface at lower dynamic heights; they result from the rapid change in temperature across the shelf-slope front. The density change, and hence the dynamic height change, across the front is small because the temperature change is largely compensated by the salinity change. As a result, synthetic temperature is very sensitive to small changes in dynamic height. Large temperature errors are also found near the core of the permanent thermocline where the vertical gradient of temperature is large. Smallest errors are found in the vicinity of the 18°C thermostad in the Sargasso Water (the region where dynamic

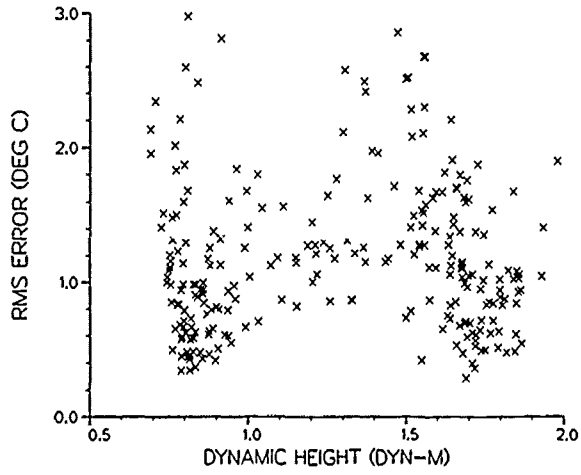

Fig. 7. Root-mean-square temperature difference between each synthetic and real profile (from *deWitt*'s [1987] monthly data sets) versus dynamic height (0/1000 dbar) for July.

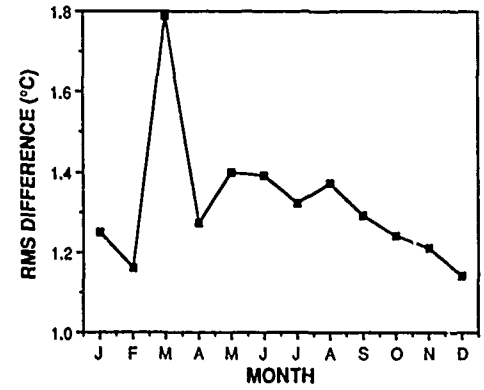

Fig. 8. Monthly rms temperature differences over all profiles and depths, between synthetic and real profiles.

heights are greater than about 1.4 dyn m), and in the North Atlantic Deep Water in the region where dynamic heights are low. Averages across dynamic height of the root-mean-square (rms) synthetic temperature change caused by surface dynamic height errors of 0.05, 0.10, 0.15, and 0.20 dyn m are shown versus depth for July in Figure 6. Mean values are about 1°C per 0.10 dyn m of height error.

Next we consider temperature differences between real and synthetic temperature profiles, where the real profiles are from *deWitt*'s [1987] monthly data sets. Dynamic heights were first computed from each real temperature and salinity profile pair, and then substituted into (1) and (2) to form the synthetic temperature profile. The rms temperature difference between each real and corresponding synthetic temperature profile (computed over 17 temperatures at standard depths between 0 and 1000 m for the July data set) is shown plotted versus surface dynamic height (0/1000 dbar) in Figure 7. The pattern shown here is typical of other months, with the smallest differences clustered on each side of the Gulf Stream front. Highest differences are found in the data sparse region within the front and at the lowest heights in the transition region between the Slope and Shelf water types. Monthly rms differences computed over all profiles and all depths are shown in Figure 8. The anomalously higher value in March is caused by intrusions of Shelf Water which sometimes overlie the Slope Water. As mentioned previously, the lower temperature of the Shelf Water is compensated by lower salinity to produce only a small change in dynamic height. In all other months, the shelf-slope front is recognizable (or missing) in these monthly data sets by a small change in dynamic height, but in March, profiles (perhaps from different years) with the same surface height may be on different sides of the front. Some dramatic cases for March have nearly identical dynamic heights but have temperature differences near 10°C in the upper 100 m. As a result, the regression relationship between the EOF mode amplitudes and the surface dynamic height represents an average of Shelf and Slope water types near the surface, and synthetic profiles produced at the low range of dynamic heights match neither water type in the upper 200 m. The anomaly in March in Figure 8 is also exaggerated because of the relatively small number of profiles used (68 compared with from 72 to 297 in the other months) and the large number of standard depths near the surface where the Shelf Water intrusions occur.

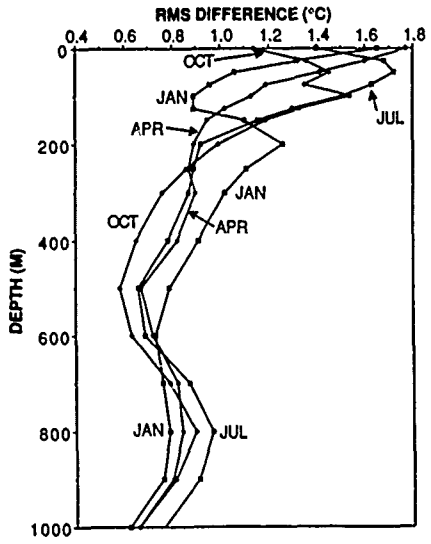

Fig. 9. Root-mean-square differences, computed over all profiles for each monthly data set, versus depth between the synthetic and real temperature profiles.

The rms temperature error versus depth between the true and synthetic profiles, is shown at 4-month intervals (January, April, July, and October) in Figure 9. In the upper 200 m, errors are between about 1°C and 2.5°C and decrease generally to about 1°C below 200 m. Seasonal differences are minor except near the surface, where errors are largest in January and April.

4. METHOD

Estimates of the geoid height along Geosat ERM ascending ground tracks were computed by Carnes et al. (1990) by two different methods using the altimeter and AXBT data sets described in section 2.

In the first method, AXBT-derived geoid profiles, denoted by $G^{\mathrm{AXBT}}(x)$, were computed along Geosat ERM ground tracks by subtracting the dynamic height anomaly at the surface relative to 3000 dbar (computed from AXBT profiles) from the corrected and adjusted altimeter-derived sea level series coincident with the AXBT section. Final series of geoid heights at approximately 7 km spacing along each ground track were computed by linear interpolation between AXBT drop positions. This resulted in from one to three AXBT geoids for each ground track, one for each AXBT section taken during the three REX AXBT surveys.

In the second method, the feature-model-derived geoids, denoted by $G^{\mathrm{FM}}(x)$, were computed as the difference between 1-year means of altimeter-derived sea level and modeled dynamic height. Three dimensional grids of temperature were first computed at 1-week intervals throughout the 1-year period using a feature-modeling approach [*Bennett et al.*, 1988] based upon climatology plus maps of the positions of the Gulf Stream and eddies. Dynamic height anomaly at the surface relative to 3000 dbar was then computed for each grid, and the average of these weekly grids were averaged to form the modeled surface topography grid.

The AXBT dynamic heights and the feature model mean dynamic heights were both first computed relative to different reference levels; AXBT heights were derived using the EOF-based regression relationships which use a 1000-dbar reference level, and the feature model heights were computed relative to 1500 dbar. An examination of Pegasus velocity profiles taken in sections across the Gulf Stream by *Halkin and Rossby* [1985] indicates that a reference level deeper than 2000 dbar should be used. We also find that surface topography gradients vary significantly with choice of reference level. Linear least squares regression of dynamic heights computed relative to different reference levels from the same 2033-profile data set used in the derivation of the EOFs yielded the following relationships:

$$d_{1500} = 0.141 + 1.091\, d_{1000}$$

$$d_{3000} = 0.712 + 1.176\, d_{1000}$$

(where d_x is dynamic height at the surface relative to x dbar) which are accurate to about 0.03 dyn m. These indicate that a 1.0 dyn m change relative to 1000 dbar is nearly a 1.18 dyn m change relative to 3000 dbar. We chose to use a 3000-dbar reference level to determine the baroclinic component of surface topography, and all heights were converted to this reference level using the above linear equations.

Estimates of the sea surface topography T were computed at each AXBT position from the concurrent altimeter data according to

$$T_i(x) = L_i^*(x) - G(x) \tag{3}$$

where x is the position (latitude) along the ground track, $L_i^*(x)$ is the adjusted sea level computed from altimeter measurements, $G(x)$ (either G^{AXBT} or G^{FM}) is the estimate of the geoid height, and the subscript i represents a particular Geosat overflight of a given ground track. The sea level was adjusted, as is discussed by Carnes et al. (1990), by first performing a correction to remove the long-wavelength radial orbit error and then by adding back an estimate of seasonal variation in sea level removed by the orbit error correction. An altimeter-derived estimate of sea surface topography was computed using the feature-modeled geoid at each of the AXBT positions taken during the three surveys. Surface topography at AXBT positions was computed with the AXBT geoids only if the AXBT geoid was computed from a different set of AXBTs. Therefore surface topography could not be computed using AXBT geoids for some AXBT sections (those where only one AXBT survey of a ground track was taken) while either one or two estimates of surface topography could be computed for others (where two or three AXBT transects of the same ground track were available).

The "ground truth" values of surface topography were estimated from AXBT profiles using the temperature EOFs and regressions relationships. The procedure consists of systematically making guesses of the true dynamic height for a given AXBT profile. A synthetic temperature profile for each dynamic height guess is formed using *deWitt*'s [1987] EOF regression relationship between dynamic height at the surface and the vertical profile of temperature. The best estimate of dynamic height is then chosen to be that which produces a temperature profile having the minimum rms difference with the AXBT temperature profile.

Synthetic temperature profiles were derived from both the altimeter-derived surface topography and the corresponding AXBT-derived surface topography using the EOFs and regression relationships. Differences between the true

TABLE 2. Root-Mean-Square Statistics of Isotherm Depth Differences Computed by Month and Isotherm From the Hydrographic Data Set Used by *deWitt* [1987]

	Isotherm θ								
	10°	11°	12°	13°	14°	15°	16°	17°	18°
Jan.	61(41)	59(36)	57(31)	59(32)	66(36)	63(45)	65(47)	72(60)	64(93)
Feb.	59(39)	55(33)	53(29)	64(30)	61(27)	54(28)	55(42)	63(60)	49(77)
March	48(38)	49(37)	64(44)	52(37)	58(27)	68(39)	72(49)	58(52)	59(73)
April	60(36)	57(32)	60(32)	64(31)	62(32)	63(41)	65(53)	71(73)	83(111)
May	58(40)	57(43)	57(37)	60(29)	59(29)	62(37)	70(52)	80(66)	80(98)
June	69(44)	67(38)	65(38)	63(35)	61(36)	61(43)	67(54)	75(64)	64(77)
July	70(39)	67(35)	67(33)	63(31)	59(32)	58(37)	60(44)	61(49)	53(59)
Aug.	62(44)	61(41)	60(36)	60(36)	59(39)	58(42)	57(45)	58(48)	49(59)
Sept.	58(31)	59(29)	58(27)	56(24)	56(24)	56(30)	57(37)	54(40)	47(55)
Oct.	59(35)	57(31)	56(27)	53(25)	52(26)	52(29)	55(34)	53(39)	47(62)
Nov.	61(41)	57(35)	54(31)	53(28)	51(28)	51(32)	56(41)	60(50)	55(72)
Dec.	51(31)	49(25)	49(23)	50(26)	52(31)	57(39)	66(49)	63(53)	61(83)

Values not in parentheses are rms$[X_\theta - S(d_T)]$, where d_T is the dynamic height (0/1000 dbar) computed for each profile from the specific volume anomaly. Values in parentheses are rms$[X_\theta - S(d_X)]$, where d_X is the dynamic height (0/1000 dbar) derived for each profile by the EOF technique.

(AXBT) temperature profiles and either of the computed synthetic temperature profiles result from a combination of inaccurate estimates of the surface dynamic height, and failure of the EOF regression relationship to represent the true profile (even if the true surface topography is used in (1) and (2)). Estimates are presented in the next section for the total altimeter-derived synthetic temperature error and of the separate contributions of its two components (dynamic height errors and EOF errors). Unfortunately, the two component errors can only be approximated. The relationships between the true dynamic height d_T and the heights estimated from altimetry (d_A) and from AXBT profiles (d_X) are given by

$$d_A = d_T + \varepsilon_A \tag{4}$$

$$d_X = d_T + \varepsilon_X \tag{5}$$

where ε_A and ε_X are dynamic height errors. Also, if X_θ is the depth of the isotherm (θ) determined from an AXBT profile, and $S_\theta(d)$ is the isotherm depth determined from the synthetic profile for a given dynamic height d, then an estimate of the mean square (ms) difference between the true isotherm depth and the altimeter-derived synthetic isotherm depth is represented by

$$ms[X_\theta^i - S_\theta^i(d_A)] \tag{6}$$

where

$$ms[V^i] = \frac{1}{N}\sum_{i=1}^{N}(V^i)^2$$

An estimate of the ms error in (6) can be computed directly from the AXBT and altimeter data sets. Approximations of the altimeter-related and the EOF-related ms isotherm depth errors, which are also computed directly from these data sets, are

$$ms[S_\theta^i(d_T + \varepsilon_X) - S_\theta^i(d_A)] \tag{7}$$

$$ms[X_\theta^i - S_\theta^i(d_T + \varepsilon_X)] \tag{8}$$

where the surface topography d_X computed from the AXBT profiles has been expanded in terms of the true topography by (5). Estimates from both (7) and (8) are contaminated by errors ε_X in surface topography computed from the AXBT profiles. However, a check for consistency can be made between our present data sets and deWitt's data set by computing the ms error given by (8) for both data sets.

An improvement to the approximation given by (7) can be made if it is assumed that the EOF-related and the altimeter-related isotherm depth errors are uncorrelated. Expanding (6) into the two components and solving for the EOF-related error results in

$$ms[S_\theta^i(d_T) - S_\theta^i(d_A)] \approx ms[X_\theta^i - S_\theta^i(d_A)] - ms[X_\theta^i - S_\theta^i(d_T)] \tag{9}$$

The first term on the right-hand side of (9) is the total error which is estimated directly from the data set, and the second term is the EOF-related error which has been estimated for each month from deWitt's data set. Table 2 lists the rms isotherm depth errors, for selected isotherms, for each of deWitt's monthly data sets computed both by the second term on the right-hand side of (9) and by (8). The true rms error (square root of the second term on the right-hand side of (9) is typically near 60 m while the error computed from (8), which uses d_X instead of d_T to compute the synthetic temperature profile, is near 30 m.

Estimates of the altimeter-derived surface topography errors, ms$[\varepsilon_A]$, cannot be made directly from our data set because the altimeter-derived surface topography d_A can be compared only with the AXBT-derived surface topography d_X, which has the error ε_X, i.e.,

$$ms[d_X - d_A] = ms[\varepsilon_X - \varepsilon_A] \tag{10}$$

An approximation can be computed with the assumption that ε_A and ε_X are uncorrelated,

$$ms[\varepsilon_A] \approx ms[d_X - d_A] - ms[\varepsilon_X] \tag{11}$$

where the first term on the right-hand side can be computed from the AXBT and altimeter data sets and the second term

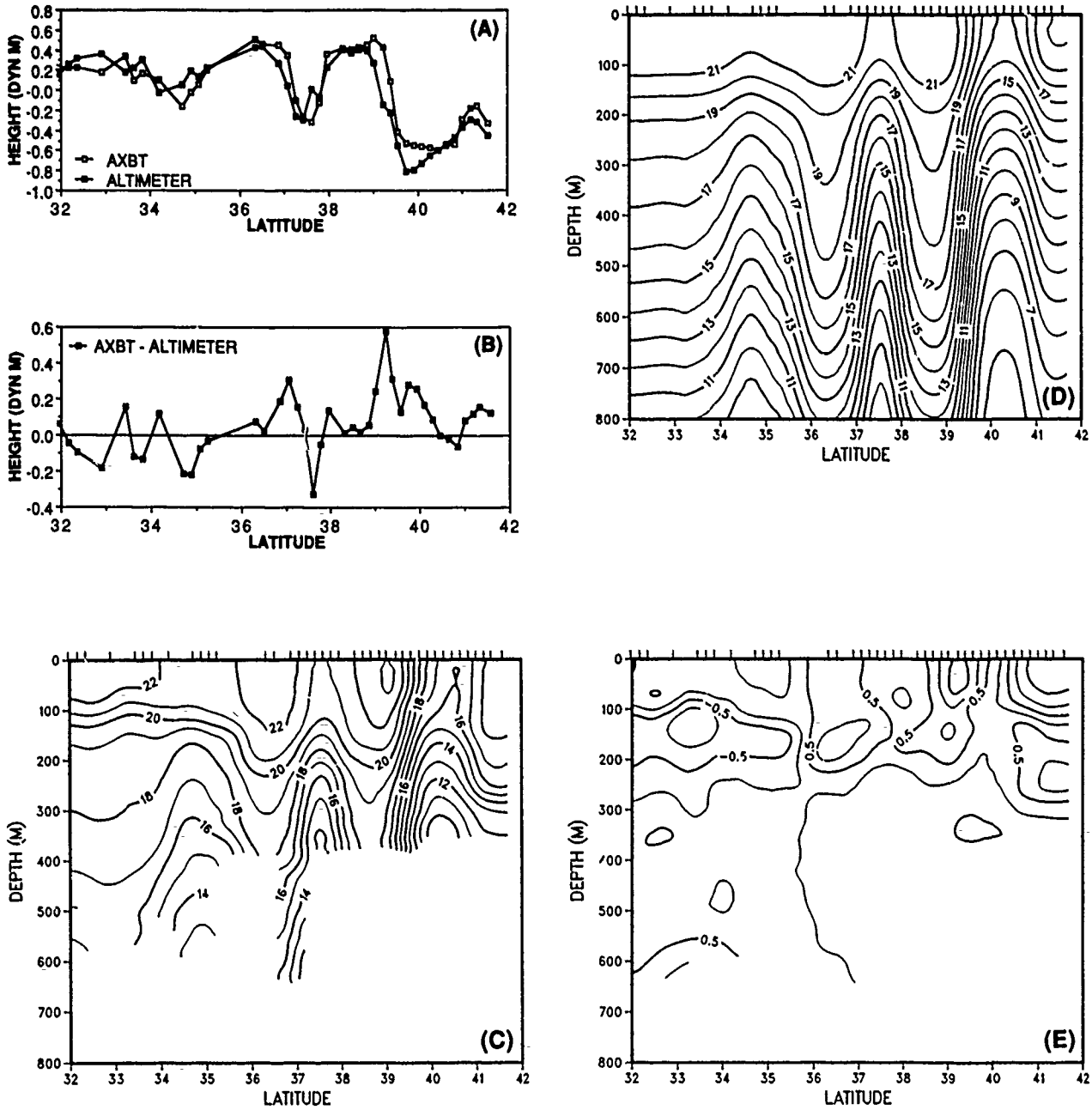

Fig. 10. Sections of (*a*) surface height, (*b*) height difference, (*c*) temperature from AXBT profiles, (*d*) temperature from synthetic profiles, and (*e*) temperature difference between AXBT and synthetic profiles for Geosat ERM ground track A6 during the December 1986 survey. The AXBT surface heights were computed using the EOF technique, and the altimeter-derived heights were computed using the feature-modeled geoid. Both were converted to a 3000-dbar reference level, and before plotting were reduced by 2.3 dyn m. Synthetic profiles were derived using the altimeter-derived heights shown. Surface height and contour plots are drawn from data only at the AXBT positions.

is estimated from deWitt's data set. Estimates of rms[ε_X] were computed in terms of dynamic height relative to 1000 dbar from *deWitt*'s [1987] data set by Carnes et al. (1990) as a function of AXBT profile length (depth). After also accounting for the errors associated with conversion from the 1000-dbar reference level to the 3000-dbar reference level using the linear relationships discussed previously, the range in errors which is dependent on profile length is approximately

$$0.07 \text{ dyn m} \leq \text{rms}[\varepsilon_X] \leq 0.12 \text{ dyn m} \qquad (12)$$

for profiles deeper than 250 m.

5. Results

Plots have been prepared of a section along one Geosat-ERM groundtrack for each AXBT survey period (December, April, and July). These transects were selected as examples because each shows several prominent features, the Gulf Stream and eddies, and because the three together span much of the east-west range of ground tracks used in this study. For each, the sea surface topography was derived by (3) using the feature-modeled geoid.

The first set (Figure 10) is from ground track A6 of the

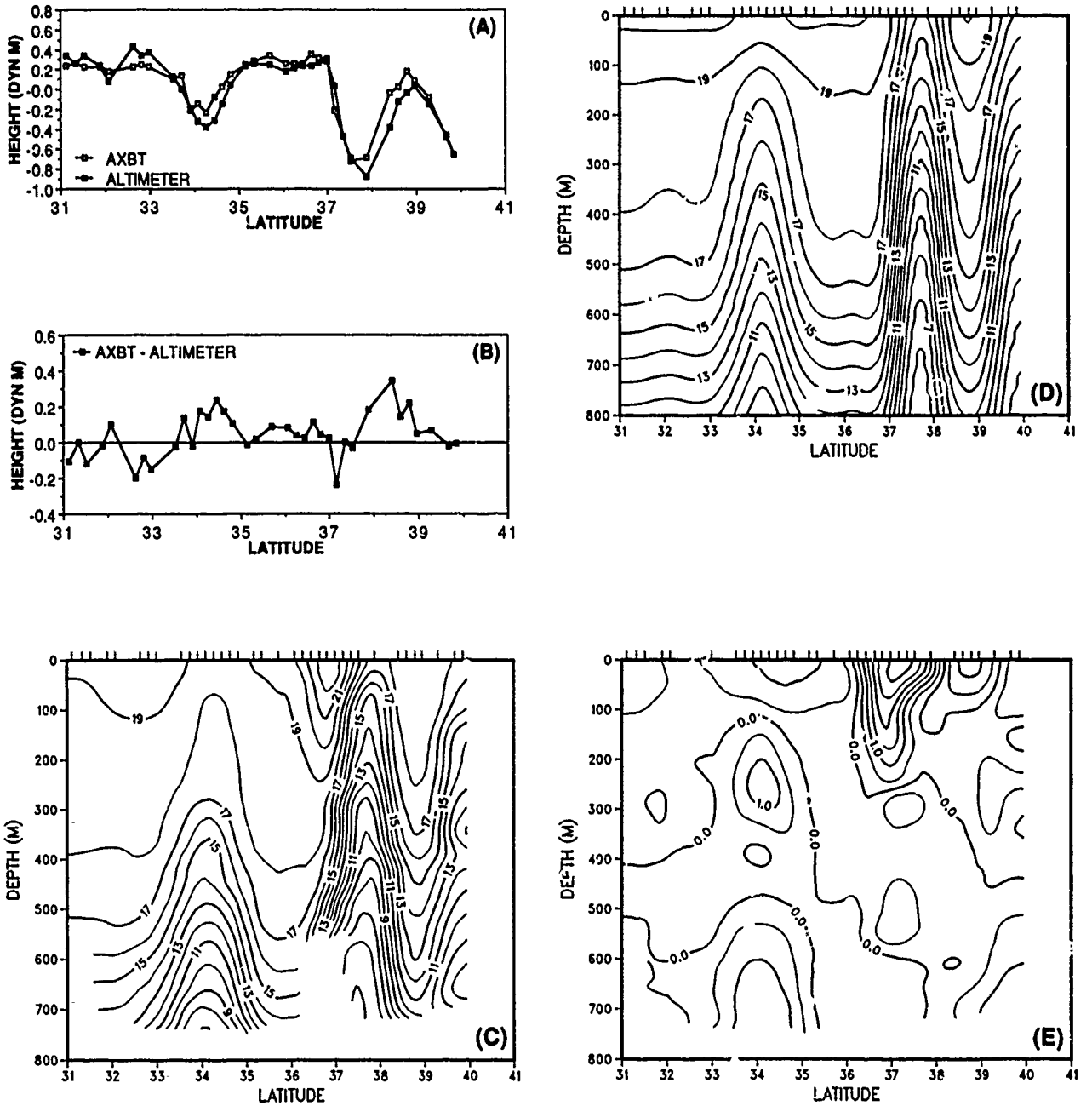

Fig. 11. Same as for Figure 10 but for ground track A1 from April survey.

December survey. Figure 10*a* shows surface topography profiles versus latitude along the ground track computed both from the altimeter data and from the AXBT profiles. The plot symbols on each graph are at the AXBT drop positions. From left to right on the graph (northward) are two cold-core Gulf Stream rings, the Gulf Stream front and then part of a warm-core ring. Though basically similar, large differences shown in Figure 10*b* between the two surface topography profiles (as great as 0.55 dyn m) occur particularly at high-gradient regions such as the Gulf Stream front and may be due partly to small shifts in the locations of the features during the 9-hour period between the Geosat overpass and the AXBT drops or to inaccuracy in the reported AXBT drop positions. Other significant differences are evident in the structure of the southern cold-core eddy and in the region between the north edge of the Gulf Stream and the warm-core eddy.

Figures 10*c* and 10*d* show the corresponding vertical section contour plots of temperature drawn from the AXBT profiles and the synthetic temperature profiles, respectively. Most AXBT profiles are only about 400 m in depth. Contours drawn deeper were computed by interpolation between profiles spaced at least 1° of latitude apart. Differences (Figure 10*e*) between these two sections can be (subjectively) classified as those related to inaccuracies in the dynamic heights (altimeter-related errors) used to calculate the synthetic temperature profiles by (1) and (2) and those due to discrepancies between the true and synthetic profiles which would be present given the true surface topography (EOF-related errors). Synthetic temperature errors resulting from

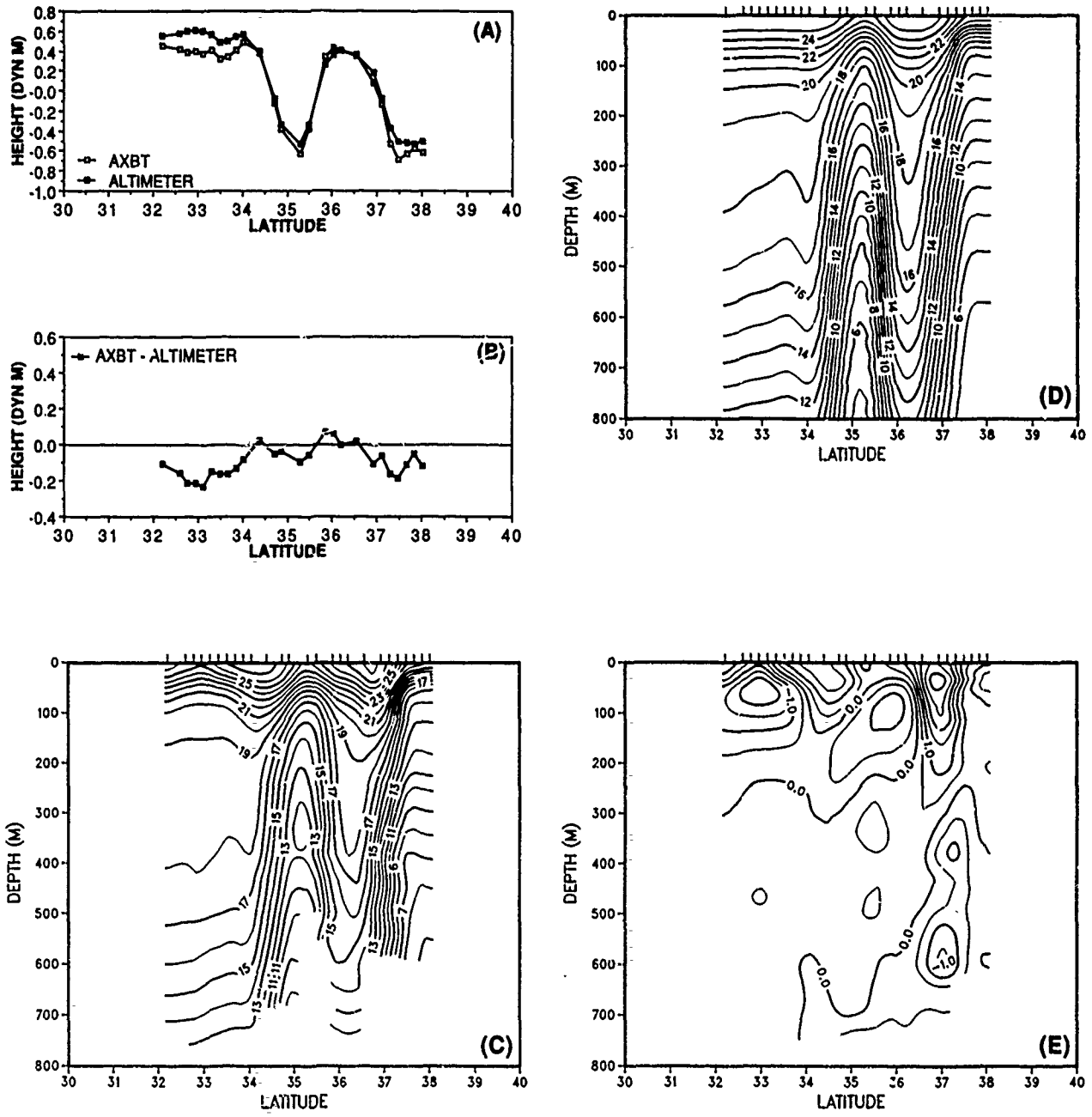

Fig. 12. Same as for Figure 10 but for ground track A242 from the July survey.

errors in dynamic height estimated from the altimeter appear to be responsible for the broadening of the southern cold-core eddy and for the disparity in the region between the north wall of the Gulf Stream and the warm-core ring. The warm core of water seen in the upper 200 m just south of the surface front of the Gulf Stream in the AXBT section is a prominent feature on nearly every section except those in July when seasonal warming of Sargasso Sea water reduces the temperature contrast. The warm core is essentially missing on all synthetic temperature sections and may be considered as an EOF-related error.

Plots from the April survey along ground track A1 are shown in Figure 11. The AXBT (d_X) and altimeter (d_A) surface topography profiles along the ground track show, from south to north, a cold-core eddy, the Gulf Stream front and a warm-core eddy. The largest height differences are found over the central and northern portions of the two eddies where the AXBT heights are higher in both case by 0.1 to 0 2 dyn m, near the center of the Gulf Stream front and near Bermuda (32.2°N). The near-surface warm-core region over the Gulf Stream seen in the AXBT vertical section (Figure 11*c*) is again missing in the synthetic section (Figure 11*d*). Another significant difference is the much thicker 18° Water thermostad [*Worthington*, 1959] over the cold-core eddy in the AXBT section as compared with the synthetic section; the 18°C isotherm depths are similar over the ring, but the 16°C isotherm depth is near 150 m on the synthetic section and near 300 m in the AXBT section at the center of the ring.

Figure 12 shows surface topography and temperature

sections along ground track A242 during the July survey. The surface topography profiles (Figure 12*a*) reveal a cold-core eddy centered near 35°N and the Gulf Stream centered near 37°N. The near-surface warm core of the Gulf Stream, evident in the AXBT section, is about 3°C warmer and is more asymmetrical than in the synthetic sections. Another major difference occurs south of the ring where the altimeter-derived heights are 0.1 to 0.2 dyn m too high, causing an erroneous 30-m to 60-m depression of the synthetic isotherms. Elsewhere, the AXBT and synthetic temperature sections are similar.

The ms error statistics defined in the previous section were computed for each AXBT transect and coincident corresponding Geosat altimeter data set. Figure 13 shows histograms prepared for the December, April, and July survey transects of the rms difference between the surface topographies computed from the AXBT profiles and those derived from the altimeter measurements, $\text{rms}[d_X - d_A] = \text{rms}[\varepsilon_X - \varepsilon_A]$. Altimeter-derived surface heights were computed using a maximum of three different geoid estimates: the feature-modeled geoid and the AXBT geoids derived for the same ground track from each of the other two AXBT surveys when available. The rms difference is typically between 0.1 dyn m and 0.2 dyn m with differences being smallest, except in three cases, when the feature model geoid is used. The rms difference for cases where the feature-modeled geoid is used is less than 0.15 dyn m on all ground tracks west of A2 but is greater than 0.15 dyn m in seven out of nine cases east of track A2. The cause of the greater rms differences toward the east has not been isolated, but it appears to be associated with larger mean offsets (averaged over all estimates for a given transect of a ground track) between the AXBT-derived and the altimeter-derived heights toward the east. Histograms of the mean difference of $d_X - d_A$ along each track (Figure 14) again show generally higher values east of track A2.

Histograms of the rms difference in the depth of the 15°C isotherm, the square root of (6) with $\theta = 15$°C, for each transect of each ground track are shown in Figure 15. Along some transects, particularly in December, too few profiles were found with a 15°C temperature at any depth, and were not included on the graph. When d_A is computed with the feature-modeled geoid, the rms difference is below 100 m in 14 out of 18 cases (9 of 18 with the AXBT geoids) and less than 60 m in half of the cases (3 of 18 with the AXBT geoids).

Table 3 lists several global rms difference statistics computed over all height or isotherm differences derived from each AXBT and corresponding altimeter measurement for all ground tracks and survey periods. The results are shown separately for the two cases where either the feature-modeled geoid or the AXBT geoid was used in the calculation of surface height from the altimeter data. Since a feature-modeled geoid is available for every track (and each survey period), but the AXBT geoids are available only for tracks where two or more AXBT surveys were made, the two sets of difference used to form the overall results are not identical. The overall rms difference between the AXBT-derived surface heights and the altimeter-derived heights (equation (10)) is 0.15 dyn m when the feature-modeled geoid is used, and 0.19 dyn m when the AXBT geoid is used. Depth differences (equations (6), (7), and (8)) were computed for the 13°C, 15°C, and 17°C isotherms. The overall depth difference between AXBT and synthetic (computed using the altimeter-derived surface height) isotherm depths ranges between 80 m and 93 m when the feature-modeled geoid is

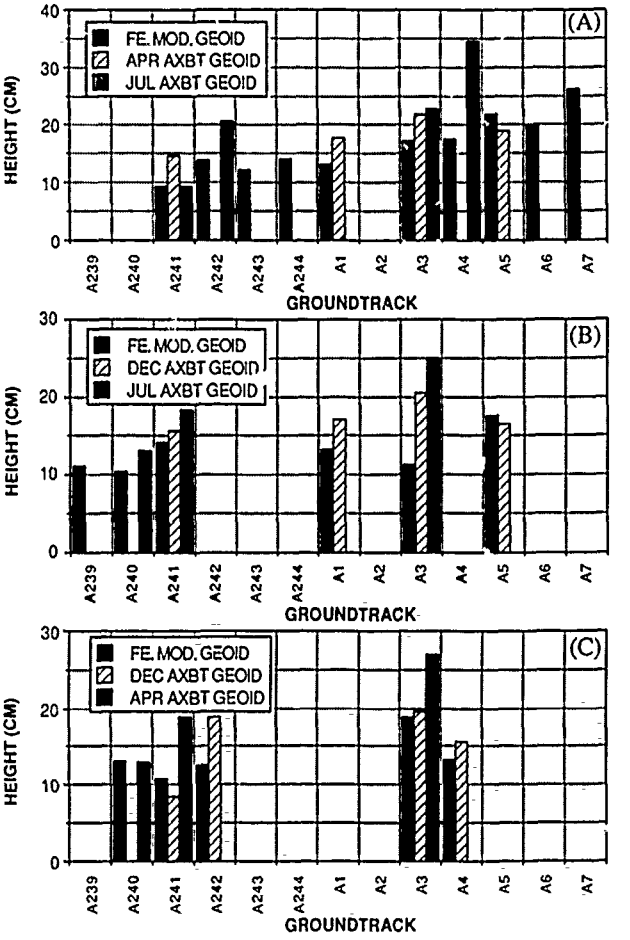

Fig 13 Histograms of the root-mean-square sea surface height difference, $\text{rms}[d_X - d_A]$, between dynamic heights computed from AXBT profiles and the surface heights computed from altimeter data. Each rms value computed using all AXBTs and corresponding altimeter measurements at the AXBT positions along a given Geosat ERM ground track and for a given AXBT survey period. (*a*) December 1986, (*b*) April 1987, (*c*) July 1987. Surface heights computed from the altimeter data employed (cases as indicated on graphs) one or more of the geoid height estimates defined in the text as the feature-modeled geoid and the December, April, and July AXBT geoids.

TABLE 3. Root-Mean-Square Statistics of Surface Height and Isotherm Depth Differences Computed Over the Entire Data Set Using All Available AXBT and Corresponding Synthetic Temperature Profiles and the AXBT-Derived and Altimeter-Derived Surface Heights

	Isotherm θ		
	13°	15°	17°
$\text{rms}[X_\theta - S_\theta(d_A)]$	93 (120)	80 (96)	90 (107)
$\text{rms}[X_\theta - S_\theta(d_X)]$	34 (30)	21 (18)	39 (35)
$\text{rms}[S_\theta(d_X) - S_\theta(d_A)]$	83 (110)	76 (96)	79 (108)

Altimeter surface heights d_A were derived using the feature-modeled geoid for the first set of results and using the AXBT geoids for the second set (in parentheses). $\text{rms}[d_X - d_A] = \text{rms}[\varepsilon_X - \varepsilon_A]$ = 0.15 (0.19). Results are in meters.

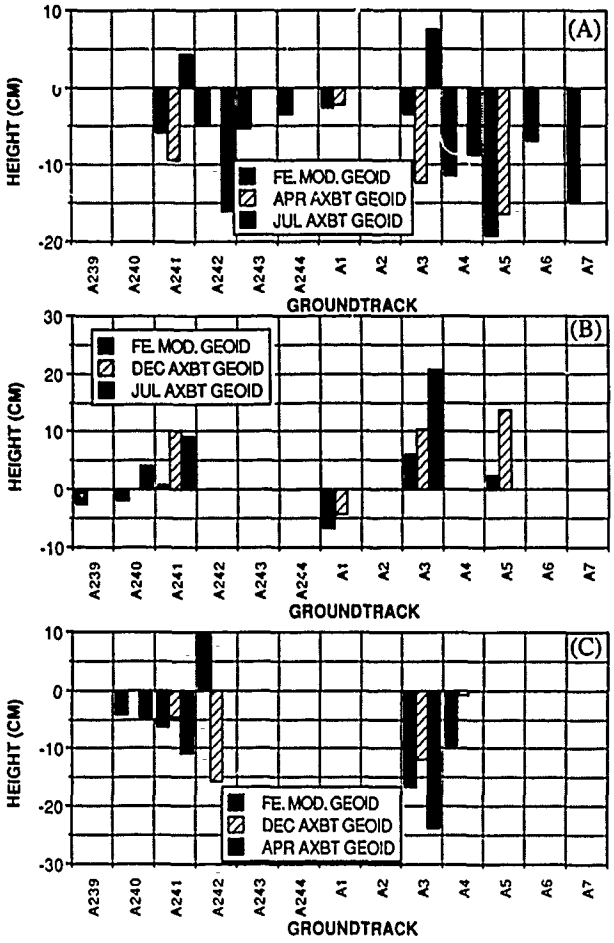

Fig. 14. Same as for Figure 13 except for the mean difference, $(1/N)\ \Sigma_{i=1}^{N}\ (d_X^i - d_A^i)$.

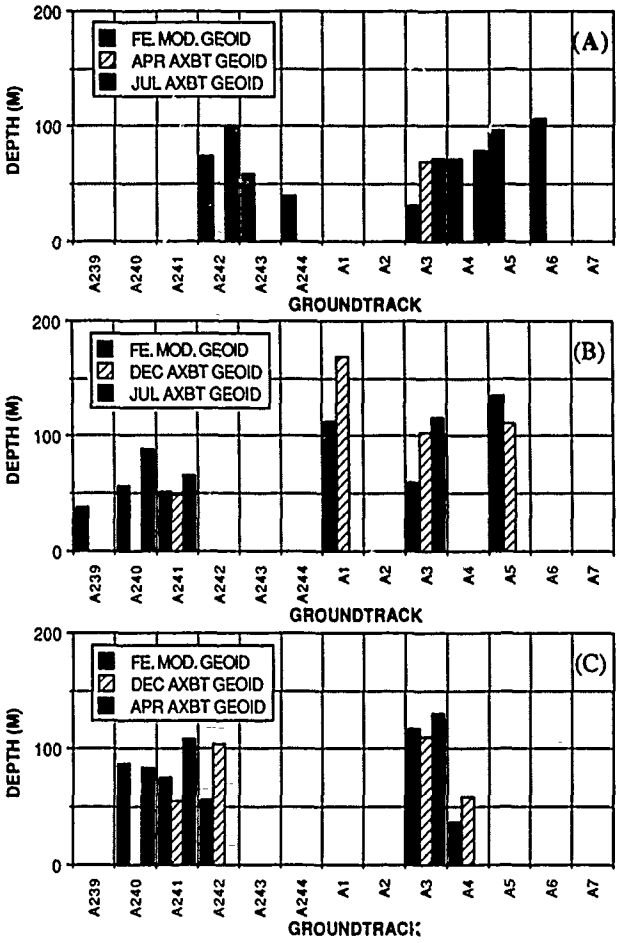

Fig. 15. Histograms of the root-mean-square 15°C isotherm depth difference, rms$[X_{15} - S_{15}(d_A)]$, between AXBT profiles and synthetic temperature profiles, where synthetic profiles were computed base on the surface heights (d_A) derived from the altimeter. Each rms value computed using all AXBTs and corresponding altimeter-derived synthetic profiles at the AXBT positions along a given Geosat ERM groundtrack and for a given AXBT survey period: (*a*) December 1986, (*b*) April 1987, (*c*) July 1987. Surface heights computed from the altimeter data employed (cases as indicated on graphs) one or more of the geoid height estimates defined in the text as the feature-modeled geoid and the December, April, and July AXBT geoids.

used and between 96 m and 120 m when the AXBT geoid is used. A large (about 60%) decrease in the rms error in the depth differences is obtained by using the AXBT-derived heights in the derivation of the synthetic profiles. However, this last result is lower than that which would be obtained by using the true surface heights in the derivation of the synthetic profiles. This is because the algorithm for computing dynamic heights from AXBT profiles chooses the height which produces the synthetic profile most similar (in a least squares sense) to the AXBT profile. All rms differences dependent upon the altimeter-derived surface heights (d_A and $S_\theta(d_A)$) are greater by 18% to 36% when the AXBT geoid is used than when the feature-modeled geoid is used.

As was stated in the preceding section, the estimates of the altimeter-derived surface height error and the altimeter-related and EOF-related (but not the total) errors in isotherm depth listed in Table 3 are all contaminated by errors in the estimates, d_X, of the true surface height d_T. Corrected values of the altimeter-derived surface height error rms$[\varepsilon_A]$, computed by (11), and of the altimeter-related isotherm depth error, computed by (9), are given in Table 4. The computed values of rms$[\varepsilon_A]$ depend upon the values selected for rms$[\varepsilon_X]$. At the center of the range of rms$[\varepsilon_X]$ given in (12), values of the rms altimeter height error are 0.12 dyn m and 0.17 dyn m for the feature-modeled geoid and AXBT geoid cases, respectively. In fact, the value of rms$[\varepsilon_X]$ does not include the dynamic height errors caused by movement of the sharp-gradient features (rings and the Gulf Stream) in the period between the AXBT drops and the Geosat altimeter overflight. Taking this factor into account would increase the values of rms$[\varepsilon_X]$ and decrease the estimate of rms$[\varepsilon_A]$. The corrected values of the altimeter-related isotherm depth error (equation (9) and Table 4) average near 60 m when the feature-modeled geoid is used. This is equivalent to the EOF-related isotherm depth error estimated from *deWitt*'s [1987] data set (Table 2); i.e., the EOF-related and altimeter-related errors contribute equally to the overall isotherm depth error.

6. Conclusion and Discussion

Our goal has been to evaluate the feasibility of recreating the three-dimensional thermal structure of the ocean for a small region encompassing the Gulf Stream using remotely sensed observations from a satellite altimeter. Synoptic

TABLE 4*a*. Estimates of the Root-Mean-Square Altimeter-Derived Surface Height Error Computed Over the Entire Available Set of Results (Table 3) and With the rms[ε_A] Estimated by (11)

	rms[ε_X]		
	0.07	0.09	0.11
Feature-modeled geoid	0.13	0.12	0.10
AXBT geoids	0.18	0.17	0.15

fields synthesized in this manner may find use in the initialization and update of circulation models and in regional acoustic assessments. The two primary components of the approach are the accurate determination of the sea surface height by altimetry and the subsequent calculation of synthetic temperature profiles from the surface heights. In this study, we have evaluated the accuracy of the altimeter-derived sea surface heights by comparison to dynamic heights computed from AXBT profiles and have shown, after accounting for the inaccuracies of the AXBT-derived dynamic heights, that the rms height error is about 0.12 dyn m. Several factors contribute to these errors: the range precision of the altimeter, the method for removing orbit errors from the sea level data, the accuracy of geoid heights, and the accuracy of the environmental corrections applied to the altimetry data, and those factors not corrected such as the water vapor error. These height errors alone result in an rms depth error for synthesized isotherms of about 60 m which is comparable to the errors made by synthesizing the temperature profiles using *deWitt*'s [1987] method when the correct dynamic height is used. If further progress were to reduce the errors in one of the components by 50%, for example, the total error would be reduced by only about 21%. Therefore substantial progress will require improvements to both components.

Surface heights and their synthesized temperature profiles computed using the feature-modeled geoid show better agreement with AXBTs than those computed with the AXBT-derived geoids. Some possible reasons are discussed by Carnes et al. (1990). An advantage of the feature-modeled geoid is that geoid heights may be computed at any location along Geosat ERM ground tracks within the model boundaries, whereas AXBT-derived geoid profiles are presently available only along a few selected ground tracks. However, our analysis has detected an apparent trend of increasing altimeter-derived height errors toward the east side of our study area, perhaps due to an offset bias of the feature-modeled geoid.

The EOF regression relationships have been shown to represent poorly some thermal features of the upper few hundred meters of the ocean such as the near-surface warm-core of the Gulf Stream and, in some cases, the near-surface region over Gulf Stream rings. In practice, synthetic temperature profiles generated from satellite altimetry will be used in conjunction with other sources of data such as surface temperatures obtained from satellite IR data, observations from ships and aircraft, and analyses from upper ocean models which also employ several environmental data types to obtain a more complete representation of the synoptic oceanic thermal field.

TABLE 4*b*. Estimates of the Root-Mean-Square Altimeter-Related Synthetic Isotherm Depth Error Computed Over the Entire Available Set of Results (Table 3) and With the rms[$S_\theta(d_I) - S_\theta(d_A)$] Estimated by (9)

	Isotherm θ		
	13°	15°	17°
Feature-modeled geoid	71	53	62
AXBT geoid	104	75	85

The EOFs and regression relationships for temperature have been computed so far only for two small domains, regions surrounding the Gulf Stream and the Kuroshio, and evaluated only for the Gulf Stream. As other regions are examined, we expect to encounter cases where the requirement for a unique relationship between dynamic height and subsurface structure is not met. Where variability in density structure is large for a given dynamic height, or where the correlation between the vertical structure of temperature and salinity is low, the synthetic profile method may be of little use. Ambiguities should generally decrease as the size of the region (over which the EOF-based relationships are derived) decreases, but the size of the region must be large enough to provide a reasonable number of profile measurements, and the measurements must encompass the full range of variability encountered within a region. In cases where changes in salinity structure are compensated by changes in temperature to produce no net change in density, the synthetic profile method will fail when the only independent variable is dynamic height. However, initial experimentation with an expanded regression analysis, where the EOF amplitudes are represented as polynomials of both dynamic height and surface temperature (also available from satellite observations of the ocean surface), results in relationships that can distinguish among different water types which have significant climatological surface temperature differences. For example, the expanded relationships reproduce the near-surface warm core of the Gulf Stream and are able to distinguish between the Shelf and Slope water types.

Acknowledgments. This paper is a contribution to the NOARL 6.2 data assimilation program sponsored by the Office of Naval Technology (program element 62435N). The AXBTs used in this study were collected as part of NOARL's Regional Energetics Experiment (REX) and were processed by Jan Dastugue and William Teague. The altimetry data were made available to us from the REX project and were edited by Jan Dastugue. NOARL contribution 322:040:89.

REFERENCES

Bennett, T. D., M. R. Carnes, P. A. Phoebus, and L. M. Reidlinger, Feature modeling. The incorporation of a front and eddy map into optimal interpolation-based thermal analysis, *NORDA Tech. Rep. 242*, 20 pp., Nav. Oceanogr. and Atmos. Res. Lab., Stennis Space Center, Miss., 1989.

Bernstein, R. L., G. H. Born, and R. H. Whritner, Seasat altimeter determination of ocean current variability, *J. Geophys. Res.*, *87*, 3261–3268, 1982.

Byrne, H. M., and P. E. Pullen, Seasat-derived surface topography: Comparison with coincident Kuroshio hydrographic data, *J. Geophys. Res.*, *88*, 2621–2625, 1983.

Cheney, R. E., Comparison data for Seasat altimetry in the western North Atlantic, *J. Geophys Res.*, *87*, 3247–3253, 1982.

deWitt, P. W., Modal decomposition of the monthly Gulf Stream/Kuroshio temperature fields, *NOO Tech. Rep. 298*, 40 pp., Nav. Oceanogr. Off., Stennis Space Center, Miss., 1987.

Fiedler, P. C., Surface manifestations of subsurface thermal structure in the California Current, *J. Geophys. Res.*, *93*, 4975–4983, 1988.

Halkin, D., and T. Rossby, The structure and transport of the Gulf Stream at 73°W, *J. Phys. Oceanogr.*, *15*, 1439–1452, 1985.

Hallock, Z. R., J. L. Mitchell, and J. D. Thompson, Sea surface topographic variability near the New England Seamounts: An intercomparison among in situ observations, numerical simulations, and Geosat altimetry from the Regional Energetics Experiment, *J. Geophys. Res.*, *94*, 8021–8028, 1989.

Hawkins, J. D., and P. M. Smith, Effects of atmospheric water vapor on the detection of mesoscale oceanographic features from Geosat, *NORDA Tech. Rep. 126*, 19 pp., Nav. Oceanogr. and Atmos. Res. Lab., Stennis Space Center, Miss., 1986.

Kao, T. W., The Gulf Stream and its frontal structure: A quantitative representation, *J. Phys. Oceanogr.*, *17*, 123–133, 1987.

Khedouri, E., and C. Szczechowski, Potential oceanographic applications of satellite altimetry for inferring subsurface thermal structure, *Oceans 83, Proc. Mar. Techol. Soc.*, 274–280, 1983.

Leitao, C. D., N. E. Huang, and C. G. Parra, A note on the comparison of radar altimetry with IR and in situ data for the detection of the Gulf Stream surface boundaries, *J. Geophys. Res.*, *84*, 3969–3973, 1979.

Mitchell, J. L., J. M. Dastugue, W. J. Teague, and Z. R. Hallock, The estimation of geoid profiles in the northwest Atlantic from simultaneous satellite altimetry and airborne expendable bathythermograph sections, *J. Geophys. Res.*, this issue.

Tapley, B. D., G. H. Born, and M. E. Parke, The Seasat altimeter data and its accuracy assessment, *J. Geophys. Res.*, *87*, 3179–3188, 1982.

Teague, W. J., A technique for processing noisy AXBT data, *NORDA Tech. Rep. 150*, 11 pp., Nav. Oceanogr. and Atmos. Res. Lab., Stennis Space Center, Miss., 1986.

Worthington, L. V., The 18° water in the Sargasso Sea, *Deep Sea Res.*, *5*, 297–305, 1959.

Wunsch, C., and E. M. Gaposchkin, On using satellite altimetry to determine the general circulation of the oceans with application to geoid improvement, *Rev. Geophys.*, *18*, 725–745, 1980.

M. R. Carnes and J. L. Mitchell, Ocean Sensing and Prediction Division, Naval Oceanographic and Atmospheric Research Laboratory, Stennis Space Center, MS 39529-5004.

P. W. deWitt, Fleet Numerical Oceanography Center, Monterey, CA 93943-5005.

(Received June 2, 1989;
accepted January 24, 1990.)